Forming the Moon from numerical simulations

Jérémy COUTURIER

May 21, 2023

Contents

Abstract

After a giant impact between the proto-Earth and a hypothetical celestial object, a disk of gas and liquid fragments is orbiting the Earth. Collisions between these moonlets and subsequent accretion are believed to have formed the Moon. In this draft, I state the mathematical model used to simulate the formation of the Moon.

In this draft, $\mathfrak{E}$ denotes the Earth and $\mathcal{O}$ is its center of mass. In a general fashion, the mass of the Earth and of the Sun are denoted $M_\oplus$ and $M_\odot$, respectively. Let N be the total number of moonlets orbiting $\mathfrak{E}$ and for $1 \leq j \leq N$, m_j is the mass of the j^{th} moonlet.

The geocentric inertial reference frame is $(\mathcal{O}, \boldsymbol{i}, \boldsymbol{j}, \boldsymbol{k})$, while the reference frame attached to the rotation of the Earth is $(\mathcal{O}, \boldsymbol{I}, \boldsymbol{J}, \boldsymbol{K})$, with $\boldsymbol{k} = \boldsymbol{K}$. The transformation from one to another is done through application of the rotation matrix $\boldsymbol{\Omega}$, which is the sideral rotation of the Earth. All vectors and matrices are bolded while their norms are unbolded.

1 Interactions with the Earth

1.1 Center of mass

The gravitational interactions between the moonlets and the center of mass of the Earth is the most obvious physical effect to take into account, as any other contribution is negligible in regards[1]. Let $\boldsymbol{r}$ be the position of a moonlet of mass m in the geocentric reference frame. Its gravitational potential per unit mass reads

$$V = -\frac{\mathcal{G}M_\oplus}{r}, \tag{1}$$

where $\mathcal{G}$ is the gravitational constant. The moonlet's acceleration is given by

$$\ddot{\boldsymbol{r}} = -\nabla_{\boldsymbol{r}} V, \tag{2}$$

that is,

$$\ddot{\boldsymbol{r}} = -\frac{\mathcal{G}M_\oplus}{r^3}\boldsymbol{r}. \tag{3}$$

1.2 Flattening

The Earth is not exactly a sphere, and under its own rotation, it tends to take an ellipsoidal shape. Let $\zeta(\theta, \varphi)$ be the altitude of the geoid of the Earth, where

$$\begin{aligned} X &= r\sin\theta\cos\varphi, \\ Y &= r\sin\theta\sin\varphi, \\ Z &= r\cos\theta, \end{aligned} \tag{4}$$

is the relation between the cartesian and spherical coordinates of $(\mathcal{O}, \boldsymbol{I}, \boldsymbol{J}, \boldsymbol{K})$. If $R_\oplus$ denotes the mean radius of the Earth, then the geoid is generally defined as the only equipotential surface such that

$$\int_0^{2\pi}\int_0^{\pi} \zeta(\theta, \varphi)\sin\theta d\theta d\varphi = R_\oplus, \tag{5}$$

[1] On short timescales, collisions and close encounters are not.

that is, as the only equipotential surface whose average over the sphere is the mean radius. Expanding the geoid over the spherical harmonics as

$$\begin{aligned} \zeta(\theta,\varphi) &= R_\oplus \left[1 + h(\theta,\varphi)\right], \\ h(\theta,\varphi) &= \sum_{l=2}^{+\infty} \sum_{m=-l}^{l} \epsilon_{lm} Y_{lm}(\theta,\varphi), \end{aligned} \tag{6}$$

satisfies Eq. (5). For reference, the spherical harmonics are defined in Appendix A of my PhD manuscript. If the Earth is spherical, then its potential is radial and we take $\zeta(\theta,\varphi) = R_\oplus$, that is, $\epsilon_{lm} = 0$ for all l and m.

Similarly to the geoid, we write the potential raised by the redistribution of mass within the Earth as (*e.g.*, Boué *et al.*, 2019)

$$\begin{aligned} V(r,\theta,\varphi) &= -\frac{\mathcal{G}M_\oplus}{r}\left[1 + \hat{v}(r,\theta,\varphi)\right] + V_\Omega(r,\theta), \\ \hat{v}(r,\theta,\varphi) &= \sum_{l=2}^{+\infty} \sum_{m=-l}^{l} \left(\frac{R_\oplus}{r}\right)^l \hat{V}_{lm} Y_{lm}(\theta,\varphi), \end{aligned} \tag{7}$$

where $V_\Omega(r,\theta) = \Omega^2 r^2 \left(P_2(\cos\theta) - 1\right)/3$ is the potential raised by the rotation itself. We denote $\Omega_\mathrm{c} = \sqrt{\mathcal{G}M_\oplus/R_\oplus^3}$ the critical rotation rate that would compensate gravity at the equator if the Earth was spherical. With this notation, the potential raised by the deformed Earth can be rewritten

$$\begin{aligned} V(r,\theta,\varphi) &= -\frac{\mathcal{G}M_\oplus}{r}\left[1 + v(r,\theta,\varphi)\right] - \frac{1}{3}\Omega^2 r^2, \\ v(r,\theta,\varphi) &= \sum_{l=2}^{+\infty} \sum_{m=-l}^{l} \left(\frac{R_\oplus}{r}\right)^l V_{lm} Y_{lm}(\theta,\varphi), \end{aligned} \tag{8}$$

where $V_{lm} = \hat{V}_{lm}$ if $(l,m) \neq (2,0)$ and

$$V_{20} = \hat{V}_{20} - \frac{1}{3}\frac{\Omega^2}{\Omega_\mathrm{c}^2}\frac{r^5}{R_\oplus^5}. \tag{9}$$

If we assume $h \ll 1$ and $v \ll 1$ (this is equivalent to $\Omega^2 \ll \Omega_\mathrm{c}^2$), then it is easy to verify, from the definition of the geoid, that (see Wahr, 1996, Sect. 4.3.1)

$$\epsilon_{lm} = V_{lm}\Big|_{r=R_\oplus}. \tag{10}$$

This gives a relation between the figure of the Earth (the geoid) and the potential raised by the redistribution of mass.

If we limit ourselves to the quadrupolar order and if we assume that the problem does not to depend on φ (axisymmetry), then all the V_{lm} and ϵ_{lm} vanish for $(l,m) \neq (2,0)$. For the fluid Earth, it can be shown (Sect. 5.2.1 of my PhD manuscript) that (Wahr, 1996, Eq. (4.24))

$$\epsilon_{20} = -\frac{5}{6}\frac{\Omega^2}{\Omega_\mathrm{c}^2}. \tag{11}$$

The J_2 coefficient is defined as $J_2 = -\hat{V}_{20}$ (with the convention of Appendix A of my PhD manuscript for the spherical harmonics). For the fluid Earth, Eqs. (9), (10) and (11) yield

$$J_2 = \frac{1}{2}\frac{\Omega^2}{\Omega_c^2}. \tag{12}$$

According to Eq. (7), a moonlet orbiting the Earth at position $\boldsymbol{r}$ in the geocentric reference frame, feels, from the equatorial bulge, the potential per unit mass[2]

$$V_{J_2} = \frac{\mathcal{G}M_\oplus R_\oplus^2}{r^3} J_2 P_2(\cos\theta). \tag{13}$$

Using the expression of the second Legendre polynomial, we can rewrite that as

$$V_{J_2} = -\frac{\mathcal{G}M_\oplus R_\oplus^2}{2r^5} J_2 \left(r^2 - 3\left(\boldsymbol{k}\cdot\boldsymbol{r}\right)^2\right). \tag{14}$$

Equation (2) gives the contribution of the equatorial bulge to the acceleration of the moonlet. Writing $\boldsymbol{r} = x\boldsymbol{i} + y\boldsymbol{j} + z\boldsymbol{k}$, we have $\boldsymbol{k}\cdot\boldsymbol{r} = z$, and then

$$\ddot{\boldsymbol{r}} = \frac{\mathcal{G}M_\oplus R_\oplus^2 J_2}{r^5}\left[\frac{15z^2 - 3r^2}{2r^2}\boldsymbol{r} - 3z\boldsymbol{k}\right]. \tag{15}$$

We extract the value of J_2 from Eq. (12). Since the young Earth had a rotation rate much larger than today's value, the effect of the equatorial bulge should play an important role in shuffling the orbits. In particular, a high value for J_2 is responsible for a $1:1$ secular resonance between the precession of the pericentre of the moonlets and the mean motion of the Sun, that happens at a few Earth radii only. See Sect. 3 for details.

1.3 Equatorial asymmetry

2 Interaction with the Sun

The interaction between a moonlet, located at $\boldsymbol{r}$, and the Sun, located at $\boldsymbol{r}_\odot$ in the geocentric reference frame can be taken into account in the model by adding to the moonlet the potential per unit mass

$$V_\odot = -\mathcal{G}M_\odot\left(\frac{1}{|\boldsymbol{r}-\boldsymbol{r}_\odot|} - \frac{\boldsymbol{r}\cdot\boldsymbol{r}_\odot}{r_\odot^3}\right). \tag{16}$$

To the quadrupolar order, this gives

$$V_\odot = -\frac{\mathcal{G}M_\odot}{2\boldsymbol{r}_\odot^3}\left(3\frac{\left(\boldsymbol{r}\cdot\boldsymbol{r}_\odot\right)^2}{\boldsymbol{r}_\odot^2} - \boldsymbol{r}^2\right). \tag{17}$$

Equation (2) yields, for the acceleration of the moonlet

$$\ddot{\boldsymbol{r}} = \frac{\mathcal{G}M_\odot}{\boldsymbol{r}_\odot^3}\left(\boldsymbol{r} - 3\frac{\boldsymbol{r}\cdot\boldsymbol{r}_\odot}{\boldsymbol{r}_\odot^2}\boldsymbol{r}_\odot\right). \tag{18}$$

[2] Due to the axisymmetry, we can go to the geocentric frame by simply removing V_Ω in Eq. (7).

For simplification, we assume that the Earth orbits the Sun on a circular trajectory. Without restraining the generality, we can assume that the Earth's longitude of the ascending node is 0 (this can be achieved by simply putting the unit vector $\boldsymbol{i}$ of the geocentric frame towards the ascending node). Similarly, for a circular orbit, we can arbitrarily choose $\omega_\odot = 0$. We denote $a_\odot$ the semi-major axis of the Earth orbit and ϵ the obliquity of the Earth. With these notations, the vector $\boldsymbol{r}_\odot$ reads

$$\boldsymbol{r}_\odot = \begin{pmatrix} x_\odot \\ y_\odot \\ z_\odot \end{pmatrix} = \begin{pmatrix} 1 & 0 & 0 \\ 0 & \cos\epsilon & -\sin\epsilon \\ 0 & \sin\epsilon & \cos\epsilon \end{pmatrix} \begin{pmatrix} a_\odot \cos\lambda_\odot \\ a_\odot \sin\lambda_\odot \\ 0 \end{pmatrix} = \begin{pmatrix} a_\odot \cos\lambda_\odot \\ a_\odot \sin\lambda_\odot \cos\epsilon \\ a_\odot \sin\lambda_\odot \sin\epsilon \end{pmatrix}, \tag{19}$$

where $\lambda_\odot = n_\odot t = t\sqrt{\mathcal{G}M_\odot/a_\odot^3}$.

3 Long-term effects on the moonlet's orbits

4 Interaction with the gas disk

Depending on the violence of the impact, the proto-lunar disk could be initially entirely made up of gas, or could contain a non-zero fraction of liquid moonlets. Then, as the disk cools down, condensation can form new moonlets to replace those that were lost by tidal disruption. The existing moonlets thus undergo drag from the remaining gas that affects their orbits.

4.1 Structure and evolution of the gas disk

A first and simple idea consists in considering that the gas disk is stationary and axisymmetric. This approximation is valid as long as the timescale of disk evolution is large compared to the timescale of formation of the Moon. The structure is determined by solving the Euler equation, and if the total mass of the gas disk is negligible with respect to that of the Earth, then the gravitational potential takes a simple form and the Euler equation can be solved explicitly in the z direction. Assuming an isothermal equation of state $p = \rho c_\mathrm{s}^2$, where $c_\mathrm{s}(r)$ is the sound speed, we find (Armitage, 2010)

$$\rho(r,z) = C(r)\exp\left[\frac{\mathcal{G}M_\oplus}{c_\mathrm{s}^2\left(r^2+z^2\right)^{1/2}}\right], \tag{20}$$

where $C(r)$ is an integration constant, ρ is the density and p is the pressure. Assuming that the disk is thin with respect to its radial extension, expanding Eq. (20) over z/r yields

$$\rho(r,z) = \rho_0(r)\exp\left(-\frac{z^2}{2h(r)^2}\right), \tag{21}$$

where $h(r) = c_\mathrm{s}(r)/\Omega(r)$ is the vertical scale-height of the disk and $\Omega(r) = \sqrt{\mathcal{G}M_\oplus/r^3}$ is the Keplerian angular frequency. The surface density of the disk is given by $\Sigma = \int_\mathbb{R} \rho(r,z)dz$. Using Eq. (21) and the identity $\int_\mathbb{R} e^{-\alpha z^2}dz = (\pi/\alpha)^{1/2}$, we find

$$\Sigma = \sqrt{2\pi}\rho_0 h, \tag{22}$$

giving a simple relation between the surface density Σ and the mid-plane density ρ_0. Along the r direction, the Euler equation reduces to

$$\frac{v_\varphi^2}{r} = \frac{\mathcal{G}M_\oplus}{r^2} + \frac{1}{\rho}\frac{dp}{dr}, \tag{23}$$

from which we can deduce that the gas does not orbit at the Keplerian speed as soon as $dp/dr \neq 0$. Choosing for the pressure a profile $p = p_0\,(r/r_0)^{-n}$, and for the sound speed a profile $c_\mathrm{s} = c_\mathrm{s}^{(0)}\,(r/r_0)^{-\beta}$ yields

$$v_\varphi = v_\mathrm{K}\left[1 - n\frac{c_\mathrm{s}^2}{v_\mathrm{K}^2}\left(\frac{r}{r_0}\right)^{-2\beta}\right]^{1/2}, \tag{24}$$

where $v_\mathrm{K} = \sqrt{\mathcal{G}M_\oplus/r}$ is the Keplerian velocity. Armitage, 2010 seems to be discarding the factor in r/r_0 in his Eq. (2.20), as he simply writes

$$v_\varphi = v_\mathrm{K}\left[1 - n\frac{c_\mathrm{s}^2}{v_\mathrm{K}^2}\right]^{1/2}. \tag{25}$$

With these profiles, the surface density Σ and aspect ratio h/r behave like

$$\frac{h(r)}{r} = \frac{h(r_0)}{r_0}\left(\frac{r}{r_0}\right)^{1/2-\beta} \quad \text{and} \quad \Sigma(r) = \Sigma_0\left(\frac{r}{r_0}\right)^{\beta-n+3/2}, \tag{26}$$

and the structure of the disk is entirely determined by choosing these two profiles.

However, these profiles do not depend on time. The differential equation that governs the evolution of the surface density $\Sigma(r,t)$ is given by Eq. (3.6) of Armitage, 2010. It cannot be solved analytically in the general case and in order not to have to numerically solve this differential equation, we add time-dependency in the model by considering the fit given by Ida *et al.*, 2020

$$\Sigma(r,t) = \Sigma_0 t_\star^{-21/22}\left(\frac{r}{R_\oplus}\right)^{-3/4}\exp\left[-\left(\frac{r}{r_\star}\right)^{5/4} t_\star^{-15/22}\right], \tag{27}$$

where Σ_0 is the surface density at $r = R_\oplus$ and $t = 0$, $r_\star$ is a typical radius and

$$t_\star = 1 + \frac{75\nu t}{16 r_\star^2}, \tag{28}$$

with $\nu \ll c_\mathrm{s}^2\Omega^{-1}$ homogeneous to a kinematic viscosity and $r_\star$ is chosen in Nakajima *et al.*, 2022 to be the Roche radius.

4.2 Gas drag

When a moonlet of mass m and radius R travels through the gas at velocity $\boldsymbol{v} = \dot{\boldsymbol{r}}$, it undergoes an acceleration due to gas drag. For very high Reynolds number, this acceleration is generally written

$$\ddot{\boldsymbol{r}} = -\frac{1}{2m}\rho_\mathrm{g} C_\mathrm{x}\pi R^2\,|\boldsymbol{v} - \boldsymbol{v}_\mathrm{g}|\,(\boldsymbol{v} - \boldsymbol{v}_\mathrm{g}), \tag{29}$$

where $\rho_g(r,z,t)$ is the density of the gas (computed from Eqs. (21), (22) and (27)), the dimensionless drag coefficient is $C_x = 0.45$ for a sphere-shaped moonlet at high Reynolds number and $\boldsymbol{v}_g$ is the velocity of the gas. If we write the position of the moonlet as $\boldsymbol{r} = x\boldsymbol{i} + y\boldsymbol{j} + z\boldsymbol{k}$, then the velocity of the gas at $\boldsymbol{r}$ is given by

$$\boldsymbol{v}_g = v_\varphi \left(-\sin\varphi\, \boldsymbol{i} + \cos\varphi\, \boldsymbol{j}\right) = v_\varphi \left(\frac{-y}{\sqrt{x^2+y^2}}\boldsymbol{i} + \frac{x}{\sqrt{x^2+y^2}}\boldsymbol{j}\right), \tag{30}$$

where we use Eq. (25) for v_φ. If we write $\boldsymbol{v} = \dot{x}\boldsymbol{i} + \dot{y}\boldsymbol{j} + \dot{z}\boldsymbol{k}$, then the relative velocity reads

$$\boldsymbol{v} - \boldsymbol{v}_g = \left(\dot{x} + \frac{y v_\varphi}{\sqrt{x^2+y^2}}\right)\boldsymbol{i} + \left(\dot{y} - \frac{x v_\varphi}{\sqrt{x^2+y^2}}\right)\boldsymbol{j} + \dot{z}\boldsymbol{k}, \tag{31}$$

and its norm is

$$|\boldsymbol{v} - \boldsymbol{v}_g| = \sqrt{v^2 + v_\varphi^2 + 2v_\varphi \frac{\dot{x}y - \dot{y}x}{\sqrt{x^2+y^2}}}. \tag{32}$$

4.3 Ionisation of the gas and truncation radius

5 Moonlet spawning

The total moonlet mass decreases over time due to moonlets being shattered by tidal forces when they pass too close to the Earth, or when they escape Earth gravity. In order to compensate the loss in total moonlets mass, there has to be a mechanism able to produce liquid mass outside the Roche radius.

5.1 Expansion of the inner fluid disk

One such mechanism is proposed by Salmon and Canup, 2012. The idea is to consider that below the Roche radius, tidal forces prevent liquids from accreting and the region $r < R_{\text{Roche}}$ is composed of a flat liquid disk. Due to viscous forces, the outer edge of this liquid disk tends to expand outward. As a results, tidal forces at the outer edge of the liquid disk become too weak to prevent aggregation and new liquid moonlets are formed. According to Goldreich and Ward, 1973, the typical size of the newly formed moonlets is

$$m_f = \frac{16\pi^4 \tilde{f}^2 \Sigma_f^3 r_{\text{out}}^6}{M_\oplus^2}, \tag{33}$$

where r_{out} is the radius of the outer edge of the liquid disk, Σ_f is its surface density (assumed independent of r) and $\tilde{f}$ is a dimensionless parameter less than 1, but not much smaller than 1. Salmon and Canup, 2012 choose $\tilde{f} = 0.3$. The mass M_f of the fluid disk varies due to liquid flowing out of the Roche radius and falling onto the Earth. The mass flowing out due to the viscous expansion at the outer edge (*resp.* at the inner edge) of the liquid disk reads

$$\dot{M}_{f,\text{outer}} = -2\pi r_{\text{out}} \dot{r}_{\text{out}} \Sigma_f \quad \left(resp.\ \dot{M}_{f,\text{inner}} = 2\pi r_{\text{in}} \dot{r}_{\text{in}} \Sigma_f\right), \tag{34}$$

where $\dot{r}_{\text{in}}$ is the inner edge. The timescale between two moonlet spawning is given by $\Delta\tilde{t} = m_f / \dot{M}_{f,\text{outer}}$. We simulate the spawning of moonlets due to viscous spreading of the

inner fluid disk by simply adding a new moonlet of mass m_f every $\Delta\tilde{t}$ on a circular and equatorial orbit, with a semi-major axis slightly larger than the Roche radius ($3R_\oplus$) and a mean anomaly chosen at random in $[0, 2\pi[$. Like Salmon and Canup, 2012, we take a moonlet out of the simulation and add its mass back in the inner liquid disk if that moonlet goes below $2R_\oplus$.

The expansion rates of the inner and outer edges of the liquid disk are given by Salmon and Canup, 2012 as

$$\dot{r}_\mathrm{in} = g(\varkappa)\dot{r}_\mathrm{out} = \frac{\nu_\mathrm{f}}{2r_\mathrm{in}\left(\varkappa - 1\right)\left(1 - g(\varkappa)\right)}, \tag{35}$$

where

$$g(\varkappa) = \frac{4\varkappa\left(\varkappa^{5/2} - 1\right) - 5\left(\varkappa^2 - 1\right)\varkappa^{3/2}}{4\left(\varkappa^{5/2} - 1\right) - 5\left(\varkappa^2 - 1\right)} \quad \text{and} \quad \varkappa = \frac{r_\mathrm{out}}{r_\mathrm{in}}. \tag{36}$$

The viscosity of the fluid disk is given by

$$\nu_\mathrm{f} = \frac{\pi^2\mathcal{G}^2\Sigma_\mathrm{f}^2}{\Omega^3}. \tag{37}$$

Through its dependency on Σ_f, the viscosity depends on time. However, Salmon and Canup, 2012 explicitly assume that ν_f does not depend on r, and we consider for Ω its value at the Roche radius, that is, $\Omega = \sqrt{\mathcal{G}M_\oplus/R_\mathrm{roche}^3}$. By assumption, $r_\mathrm{in} = R_\oplus$ and $r_\mathrm{out} = R_\mathrm{roche}$, which yields $\varkappa = 2.9$. We obtain

$$\dot{M}_\mathrm{f,outer} = 0.994894\nu_\mathrm{f}\Sigma_\mathrm{f}, \quad \dot{M}_\mathrm{f,inner} = 0.600914\nu_\mathrm{f}\Sigma_\mathrm{f}, \quad \text{and} \quad \dot{M}_\mathrm{f} = 1.595808\nu_\mathrm{f}\Sigma_\mathrm{f}. \tag{38}$$

The inner fluid disk surface density Σ_f cancels out from the expression of $\Delta\tilde{t}$, which means that $\Delta\tilde{t}$ does not depend on time. Assuming $R_\mathrm{roche} = 2.9R_\oplus$, a moonlet spawns from the inner fluid disk every

$$\Delta\tilde{t} = \frac{m_\mathrm{f}}{\dot{M}_\mathrm{f,outer}} = \frac{16\pi^2\tilde{f}^2}{0.994894\,\Omega} = 11.228001\,T, \tag{39}$$

where $T = 2\pi\sqrt{R_\oplus^3/\left(\mathcal{G}M_\oplus\right)}$ is the orbital period at Earth's surface. The surface of the inner fluid disk is $S_\mathrm{f} = \pi\left(R_\mathrm{roche}^2 - R_\oplus^2\right) = 7.41\pi R_\oplus^2$ and the mass of the spawned moonlets can be rewritten

$$\frac{m_\mathrm{f}}{M_\oplus} = 6.613719\frac{M_\mathrm{f}^3}{M_\oplus^3} \quad \Rightarrow \quad \frac{R_\mathrm{f}}{R_\oplus} = 1.877076\frac{M_\mathrm{f}}{M_\oplus}\left(\frac{\rho_\oplus}{\rho}\right)^{1/3}. \tag{40}$$

While the time $\Delta\tilde{t}$ between two moonlet spawning does not depend on time, the radius R_f and mass m_f of the spawned moonlets depend on time through their dependency on the mass M_f of the inner fluid disk.

5.2 Condensation of the gas disk

6 Detecting close encounters

All the physical effects mentionned so far can be treated in a straightforward manner in a time proportionnal to the total number of moonlets N, that is, if only these effects were to be taken into account, each time step would have a time complexity $\mathcal{O}(N)$.

However, it is clear that no simulation of satellite formation can reach any satisfying degree of realism without taking into account close encounters between moonlets, and in particular collisions and accretion. Furthermore, we can expect the total number of moonlets in the early stages of the proto-satellite disk to be very large, and a realistic simulation would preferably feature a large number of moonlets. The necessity of treating close encounters in an efficient time manner is thus crucial, in order not to ruin the simulation runtime.

6.1 Common algorithms

6.1.1 Brute-force $\mathcal{O}(N^2)$ algorithm

The naive algorithm consists of course in computing all $N(N-1)/2$ mutual distances and to deduce, at a given timestep, which moonlets are in a close encounter and need special treatment. This however yields a $\mathcal{O}(N^2)$ time complexity, limiting the total number of moonlets to a few thousands at best ($N \sim 2000$ in Salmon and Canup, 2012).

6.1.2 Plane-sweep algorithm and octree

Rein and Liu, 2012 propose for REBOUND two time-efficient algorithms to take care of close encounters. The first one consists in putting the moonlets in a recursive structure called octree, which allows for a treatment in $\mathcal{O}(N \ln N)$ (Barnes and Hut, 1986), but at the cost of a complicated data structure (see Rein and Liu, 2012, Sect 5.2).

The other algorithm they propose, first described by Bentley and Ottmann, 1979, consists in sweeping the space $\mathbb{R}^3$ with a plane (*e.g.* a plane $x = \text{cst}$), and to look for close encounters only between particules whose trajectory over the last timestep crosses the same x-plane. This yields a $\mathcal{O}(NK(N))$ algorithm, where $K(N) \leq N$. The algorithm is efficient when the direction of the sweep is much larger than the other two directions ($K(N) \ll N$). For a very scattered moonlet disk though, the version of the algorithm described by Rein and Liu, 2012 is inefficient. It can be improved to $\mathcal{O}(N \ln K(N))$ by following the original description of Bentley and Ottmann, 1979, but at the cost of a complicated-looking implementation. Even if an initially thin moonlet disk is simulated, for which the plane-sweep algorithm can be efficient, orbit-shuffling should eventually scatter the moonlets. The plane-sweep algorithm does not detect all collisions, but only most of them.

6.2 Closest-pair problem and collision detection

The three aforementionned algorithms are basically the only algorithms used in celestial mechanics for collision detection in N-body simulations (I think). There exist, however, other algorithms that treat the closest-pair problem, which is not unrelated to the problem of detecting all close encounters. I present here two algorithms that solve the closest-pair problem and in Sect. 6.2.3, I present a simplified, modified version of the algorithm presented in Sect. 6.2.2 that allows for collision detection in the Moon-forming disk in an efficient time manner.

6.2.1 Divide and conquer $\mathcal{O}(N \ln N)$ algorithm

The most famous efficient algorithm that solves the closest-pair problem is the divide and conquer algorithm.

The algorithm is as follow. The N moonlets are sorted according to, let's say, their x-coordinate, and recursively divided into two sets at the median value of their x, until each set contains very few moonlets and can be taken care of efficiently with a brute-force method. It turns out (see here or here) that once the closest pair of each half is found, the overall closest-pair can be found in $\mathcal{O}(N)$. If $T(N)$ denotes the time-complexity of this algorithm, we thus have

$$T(N) = 2T(N/2) + \mathcal{O}(N), \tag{41}$$

which yields $T(N) = \mathcal{O}(N \ln N)$.

6.2.2 Randomized sieve $\mathcal{O}(N)$ algorithm

Khuller and Matias, 1995 presented a randomized sieve algorithm that can solve the closest-pair problem in linear time, at the cost of dealing with a hash structure (and of using the floor function, but I don't know why this is relevant). I think that this algorithm has never been used in celestial mechanics in order to treat collisions and close encounters, but this needs to be verified. We define $\mathcal{S}_0$ as the set of all the moonlets. Let $\mathfrak{m}_1$ and $\mathfrak{m}_2$ be the two closest moonlets of $\mathcal{S}_0$ and δ the distance between them. The algorithm presented by Khuller and Matias, 1995 is only valid in two dimensions, and I present here a slightly different version that works in three dimensions. The algorithm is made of two distinct steps, although somewhat similar.

- In the first step, called *filtering* by the authors, a $\mathcal{O}(N)$ procedure is used to find an approximation $\hat{\delta}$ of δ such that $\hat{\delta}/2\sqrt{3} \leq \delta \leq \hat{\delta}$.
- Then, in the second step, this approximation is used to find δ and the pair $(\mathfrak{m}_1, \mathfrak{m}_2)$ in $\mathcal{O}(N)$ time.

For the two steps to be described, the notion of neighborhood has to be defined. Let γ be a positive non-zero real number. Imagine you have a γ-mesh of $\mathbb{R}^3$, that is, $\mathbb{R}^3$ is divided into cubes of side-length γ, with the origin being located at the junction between 8 cubes (See Fig. 1 of Khuller and Matias, 1995, for the 2-dimensional case).

Definition The neighborhood of a moonlet $\mathfrak{m}$ is defined as the cubic cell containing $\mathfrak{m}$, plus the 26 adjacent cells. It is easy to verify that:

- If a moonlet is more than $2\sqrt{3}\,\gamma$ apart from $\mathfrak{m}$, then it is not in its neighborhood.
- If a moonlet is less than γ apart from $\mathfrak{m}$, then it is in its neighborhood.

The *filtering* step consists in sieving $\mathcal{S}_0$ by a sequence $(\mathcal{S}_i)_{i\in\mathbb{N}}$ of decreasing cardinal, such that, for a particular integer $\hat{\imath}$

$$i > \hat{\imath} \quad \Rightarrow \quad \mathcal{S}_i = \emptyset. \tag{42}$$

The sieving process is as follow: In the set $\mathcal{S}_i$, pick a moonlet at random and compute the minimal distance δ_i between that moonlet and any other moonlet. Build a δ_i-mesh

and construct $\mathcal{S}_{i+1}$ by removing from $\mathcal{S}_i$ all moonlets alone in their neighborhood. Keep going until you reach the empty set. While δ_i can be computed in $\mathcal{O}(|\mathcal{S}_i|)$ time with a brute-force method, constructing $\mathcal{S}_{i+1}$ in $\mathcal{O}(|\mathcal{S}_i|)$ time requires the use of a hash structure that stores all non-empty cells of the mesh. We define $\hat{\delta} = \delta_{\hat{\imath}}$ and it is easy to prove that $\hat{\delta}/2\sqrt{3} \leq \delta \leq \hat{\delta}$.

The second step is as follow: Build a $\hat{\delta}$-mesh. Since $\delta \leq \hat{\delta}$ the two closest moonlets are in each other neighborhood. Additionally, since $\hat{\delta} \leq 2\sqrt{3}\delta$, the moonlets are expected to have at most very few moonlets in their neighborhood ($\mathcal{O}(1)$ moonlets). For each moonlet, find all moonlets in its neighborhood and compute their mutual distance to find the pair of closest moonlets.

It is clear that the second step can be performed in $\mathcal{O}(N)$. Furthermore, Khuller and Matias, 1995 showed that

$$\mathbb{E}\left(\sum_{i=0}^{\hat{\imath}} |\mathcal{S}_i|\right) \leq 2N, \tag{43}$$

where $\mathbb{E}$ denotes the expectancy. As long as $\mathcal{S}_{i+1}$ can be deduced from $\mathcal{S}_i$ in $\mathcal{O}(N)$ time, the overall complexity of the algorithm is $\mathcal{O}(N)$.

6.2.3 Simplified $\mathcal{O}(N)$ mesh algorithm for collision detection

The algorithm described by Khuller and Matias, 1995 is not completely straightforward to implement and only allows for the closest pair of moonlet to be identified. Here, I describe an algorithm inspired by that of Khuller and Matias, 1995, easier to implement and able to detect almost all collisions in $\mathcal{O}(N)$ time.

The algorithm is as follow: For a real number $\gamma > 0$, we build a γ-mesh. At each timestep, we only look for collisions between moonlets that are in each other neighborhood. If γ is chosen as a function of N and such that, on average, each moonlet has very few moonlets in its neighborhood, then the algorithm runs in $\mathcal{O}(N)$ time.

If γ is too large, the moonlets have, on average, too many other moonlets in their neighborhood, which leads to a bad time complexity. On the other hand, if γ is too small, some moonlets could be larger than γ, or could travel a distance larger than γ during a timestep. In both cases, some collisions are missed. Hence there exists an optimal choice for γ that ensures both the efficiency of the algorithm and a low time complexity.

Let us assume that, initially, all the moonlets are located in a disk of constant aspect ratio h/r, at a radius $r \leq R_{\max}$. Then they occupy a volume

$$\mathcal{V} = \frac{4}{3}\pi R_{\max}^3 \sin\varsigma = \frac{4}{3}\pi R_{\max}^3 \sqrt{\frac{h^2/r^2}{1+h^2/r^2}}, \tag{44}$$

where $\tan\varsigma = h/r$. In order for each moonlet to have, on average, at most x moonlets in its neighborhood, the mesh size must verify $(3\gamma)^3 \leq x\mathcal{V}/N$, that is

$$\gamma \leq \left(\frac{4\pi x}{81N}\right)^{1/3} \left(\frac{h^2/r^2}{1+h^2/r^2}\right)^{1/6} R_{\max}. \tag{45}$$

With $h/r = 0.05$, $R_{\max} = 10R_\oplus$, $N = 10^5$ and $x = 1$, this gives $\gamma = 0.04263R_\oplus$, or $\gamma = 271.6$ km. If the N moonlets have, let's say, a total mass that of the Moon, then their

average radius is $R = R_{\mathbb{Q}}\,/N^{1/3}$. For $N = 10^5$ this gives $R = 37.4$ km. The condition that the moonlets are smaller than γ is $2R \leq \gamma$. Choosing $x = 1$ and $R_{\max} = 10R_{\oplus}$, this gives

$$\sin\varsigma = \sqrt{\frac{h^2/r^2}{1+h^2/r^2}} \geq \frac{162}{\pi x}\left(\frac{R_{\mathbb{Q}}}{R_{\max}}\right)^3 \approx 0.0010457, \tag{46}$$

that is $h/r \gtrsim 10^{-3}$. Choosing for γ the critical value given by Eq. (45), and for h/r a value much larger than that predicted by Eq. (46) should ensure that for most of the moonlets, the simplified sieve algorithm will efficiently detect the collisions.

The largest moonlets of the simulation, however, are likely to be larger than γ. Let $\mathcal{B}$ denote the set of all moonlets larger than γ. This idea is to treat differently a moonlet according to whether or not it is in $\mathcal{B}$. If a moonlet belongs to $\mathcal{B}$, then at each timestep, we compute all the mutual distances between moonlets of $\mathcal{B}$ and any other moonlets to look for collision. If b denotes the cardinal of $\mathcal{B}$, then the time complexity is $\mathcal{O}(bN)$, and b needs to be much smaller than N for time efficiency. If a moonlet is not in $\mathcal{B}$, we treat it with the simplified sieve algorithm.

7 Resolving collision

In this section, we consider the collision between two moonlets of masses m_1 and m_2 and radii R_1 and R_2. The positions and velocities of the moonlets, at the instant of the impact, are denoted by $\boldsymbol{r}_1$, $\boldsymbol{r}_2$, $\boldsymbol{v}_1$ and $\boldsymbol{v}_2$. We also denote

$$\Delta\boldsymbol{r} = \boldsymbol{r}_1 - \boldsymbol{r}_2 \quad \text{and} \quad \Delta\boldsymbol{v} = \boldsymbol{v}_1 - \boldsymbol{v}_2. \tag{47}$$

7.1 Elastic collision

Let us first assume that the collision is elastic, in the sense that it conserves both energy and momentum. Let $\boldsymbol{v}_1'$ and $\boldsymbol{v}_2'$ be the moonlets velocities after the impact. If we write

$$\boldsymbol{v}_1' - \boldsymbol{v}_1 = -\frac{\boldsymbol{J}}{m_1} \quad \text{and} \quad \boldsymbol{v}_2' - \boldsymbol{v}_2 = \frac{\boldsymbol{J}}{m_2}, \tag{48}$$

then it is immediate to verify that the total momentum is conserved, whatever the vector $\boldsymbol{J}$ is. Let us write

$$\boldsymbol{J} = \alpha_{\text{el}}\,(\Delta\boldsymbol{r}\cdot\Delta\boldsymbol{v})\,\Delta\boldsymbol{r}, \tag{49}$$

where α_{el} is a real number. The scalar product $\Delta\boldsymbol{r}\cdot\Delta\boldsymbol{v}$ traduces the violence of the impact, in the sense that, for a grazing collision, $\Delta\boldsymbol{r}\cdot\Delta\boldsymbol{v} = 0$, while for a frontal collision, it reaches an extremum $\Delta\boldsymbol{r}\cdot\Delta\boldsymbol{v} = -\Delta r\Delta v$. The variation of kinetic energy ΔE at the impact reads

$$\Delta E = \alpha_{\text{el}}\,(\Delta\boldsymbol{r}\cdot\Delta\boldsymbol{v})^2\left(\frac{m_1+m_2}{2m_1m_2}\alpha_{\text{el}}\Delta r^2 - 1\right). \tag{50}$$

At the impact, we have $\Delta r = R_1 + R_2$ and the elasticity of the collision reads

$$\alpha_{\text{el}} = \frac{2m_1m_2}{(m_1+m_2)\,(R_1+R_2)^2}. \tag{51}$$

7.2 A model for inelastic collisions

Sect. 7.2 is now deprecated. The code does not use it. Refer to Sect. 7.3 instead.

Clearly, considering elastic collisions is not realistic enough as it prevents accretion and moonlet growth. We need to develop a model for non-elastic collisions.

7.2.1 Accretion

The results of Sect. 7.1 suggest a very straightforward model for non-elastic collisions. We simply write $\boldsymbol{J} = \alpha\,(\Delta\boldsymbol{r}\cdot\Delta\boldsymbol{v})\,\Delta\boldsymbol{r}$, and if we choose for α a non-zero value different from that given in Eq. (51) for $\alpha_{\rm el}$, then the collision in inelastic. Let us write

$$\alpha = \frac{f m_1 m_2}{(m_1+m_2)\,(R_1+R_2)^2}, \tag{52}$$

where $f \in \mathbb{R}$. Then the variation in kinetic energy due to the impact reads

$$\Delta E = 2f\,(f-2)\,\frac{m_1 m_2}{m_1+m_2}\cos^2\theta\Delta v^2, \tag{53}$$

where $\sin\theta = b/\,(R_1+R_2)$ and b is the impact parameter[3]. To prevent an energy increase, we must consider $0 < f < 2$. The condition that the two moonlets gets farther away after the impact reads $\Delta\boldsymbol{v}'\cdot\Delta\boldsymbol{r} \geq 0$. We have

$$\Delta\boldsymbol{v}'\cdot\Delta\boldsymbol{r} = (1-f)\,(\Delta\boldsymbol{v}\cdot\Delta\boldsymbol{r})\,, \tag{54}$$

and so we must take $f \geq 1$, otherwise the moonlets keep getting closer after the collision and enter each other. The relative velocity $\Delta v'$ after the impact is given by

$$\Delta v'^2 = \Delta v^2\left(1 + f\,(f-2)\cos^2\theta\right), \tag{55}$$

and choosing $f = 1$ is also unrealistic as it yields a 0 relative velocity after a frontal collision ($\theta = 0$). Therefore, we have to choose $1 < f < 2$ for a realistic inelastic collision. The quantity f parameterizes the inelasticity of the collision, with values of f close to 2 corresponding to almost elastic collisions, whereas values close to 1 correspond to very inelastic collisions.

The accretion process is managed differently according to whether or not the mutual gravitational interactions between the moonlets are taken into account.

- If the mutual gravitational interactions are considered, then we just leave the moonlets evolve after the collision. If they can't escape each other gravity, then they will just bounce back several times until they almost stop relative to each other. After a collision, we say that two moonlets merge if their relative speed is much smaller than their mutual escape velocity (say less than $0.05\,v_{\rm esc}$). The main advantage of this procedure is that it fully and realistically simulates the tidal forces that exists between the moonlets, due to the differential attraction of the Earth.

[3] This gives $\cos^2\theta = 1 - b^2/\,(R_1+R_2)^2$.

- If the mutual gravitational interactions are not considered, then the moonlets merge if their relative velocity after the impact is less than their mutual escape velocity. Such a procedure doesn't take into account tidal forces due to the Earth, and the merging criterion should probably be modified like in Appendix D of Salmon and Canup, 2012, for a better description.

7.2.2 Splitting

Previous works do not consider the possibility that, upon impact with another moonlet, a moonlet might split into two or more parts. Since the moonlets have no internal cohesion and are held only by their own gravity, such event seems likely to happen, especially for near-frontal, high-velocity impacts.

A precise description of the phenomenon seems difficult to achieve, and to simplify, we consider in this work that only the largest of the two colliding moonlets can split, into at most two parts. Let m and R be the mass and radius of that moonlet. Before the split, the potential energy of auto-gravitation is

$$U^{(0)} = -\frac{3}{5}\frac{\mathcal{G}m^2}{R}. \tag{56}$$

If the moonlet splits into two equal-sized parts, the potential energy becomes

$$U^{(1)} = -\frac{6}{5}\frac{\mathcal{G}m'^2}{R'} - \frac{\mathcal{G}m'^2}{2R'}, \tag{57}$$

where $m' = m/2$ and $R' = R/2^{1/3}$. The amount of energy needed for the split thus reads

$$U^{(1)} - U^{(0)} = \frac{3 - 2^{-8/3}\,17}{5}\,\frac{\mathcal{G}m^2}{R} \approx 0.0645335538\,\frac{\mathcal{G}m^2}{R}. \tag{58}$$

The energy ΔE lost during the impact is shared between heating and splitting. If we say that a proportion $\hat{f}$ of ΔE is splitting energy, and a proportion $1 - \hat{f}$ of ΔE is heating energy, then the splitting criterion reads

$$\hat{f}\Delta E \geq U^{(1)} - U^{(0)}, \tag{59}$$

where ΔE is given by Eq. (53). I still don't know how to deal with the splitting procedure, in particular, what velocity to give to the two parts ? I can't give them the same velocity, otherwise they will just merge right after the split, and if I give them a velocity with some angle with respect to the velocity predicted by Eq. (48), then then total angular momentum won't be conserved at the collision.

7.3 Fragmentation

The description made in Sect. 7.2.2 is too uncertain. I rely in this section on the literature to achieve the best possible description of moonlet fragmentation. We consider the collision between two moonlets, and in a similar fashion as the literature does, we refer to the largest one as the target and to the smallest one as the impactor. The impactor (*resp.*

target) has mass and radius denoted by m_1 and R_1 (*resp.* m_2 and R_2), and like in previous sections, the relative velocity at the impact is denoted by Δv, while the impact angle is

$$\theta = \arcsin\left(\frac{b}{R_1 + R_2}\right) = \arccos\sqrt{1 - \frac{b^2}{(R_1 + R_2)^2}}, \tag{60}$$

with b the impact parameter. Both moonlets share the same density ρ, and we denote $M = m_1 + m_2$.

7.3.1 Dimensional analysis

Since the moonlets are made up of liquid silicates, we make here the assumption that they have no internal cohesion and are held only by gravity. The impactor and target are entirely determined by their radius and density. Therefore, any unknown quantity X depending on the outcome of the collision follows a relation of the form

$$X = f(R_1, R_2, \rho, \Delta v, \mathcal{G}), \tag{61}$$

where f is any function. In order to simplify the problem, the literature assumes that the impactor is entirely determined by a unique scalar quantity, called the coupling parameter. This coupling parameter generally takes the form (Holsapple and Housen, 1986)

$$C = R_1 \Delta v^\mu \rho^\nu, \tag{62}$$

where μ and ν are exponents to be fitted. If, for example, $\mu = 2\nu = 2/3$, then the impactor is entirely determined by its kinetic energy and such regime is called energy scaling. The case $\mu = \nu = 1/3$ corresponds to momentum scaling and μ has been observed to lie between $1/3$ and $2/3$.

Equation (61) now reads $X = f(C, R_2, \rho, \mathcal{G})$, and in the particular case where $X = C$, we can write

$$C = f(R_2, \mathcal{G}, \rho). \tag{63}$$

We loosely use the letter f to denote a functional dependency, and f refers to distinct functions in the different equations of this section. Dimensional analysis and the π-theorem allow Eq. (63) to be rewritten as

$$f(\tilde{\Pi}_\mathrm{G}) = 0, \tag{64}$$

where

$$\tilde{\Pi}_\mathrm{G} = \frac{\mathcal{G}^\mu \rho^{\mu+2\nu} R_2^{2(\mu+1)}}{C^2} \tag{65}$$

is a dimensionless quantity. Instead of the coupling parameter C, the literature prefers to make use of the specific kinetic energy defined as (Suetsugu *et al.*, 2018, Eq. (1))

$$Q_\mathrm{R} = \frac{1}{2}\frac{m_1 m_2}{(m_1 + m_2)^2}\Delta v^2. \tag{66}$$

When the target is much more massive than the impactor, Q_R reduces to the impactor's kinetic energy per unit target mass. In that case, we can redefine the dimensionless parameter as (Holsapple and Housen, 1986, Eq. (23))

$$\Pi_\mathrm{G} = Q_\mathrm{R}\,(\rho\mathcal{G})^{-3\mu/2}\, R_2^{-3\mu} \Delta v^{3\mu-2} = \tilde{\Pi}_\mathrm{G}^{-3/2}. \tag{67}$$

Holsapple and Housen (1986) use the π-theorem to give general functional dependencies of the distribution of fragment sizes, the mass of the largest fragment and to define a fragmentation threshold.

- **Distribution of fragment sizes** Let M_m be the total mass of all fragments with mass at most m. Then there exists a function f such that

$$\frac{M_m}{M} = f\left(\frac{m}{M}, \Pi_{\rm G}\right) \tag{68}$$

- **Mass of the largest fragment** Let $\tilde{m}$ be the mass of the largest fragment remaining after the collision. By definition, $M_{\tilde{m}}/M = 1$, and so we have

$$\frac{\tilde{m}}{M} = f(\Pi_{\rm G}). \tag{69}$$

- **Threshold for catastrophic fragmentation** In the literature (Holsapple and Housen, 1986; Benz and Asphaug, 1999; Genda *et al.*, 2017; Suetsugu *et al.*, 2018), a collision is said to be catastrophic or disruptive (*resp.* erosive or cratering) if $\tilde{m} \leq M/2$ (*resp.* if $\tilde{m} \geq M/2$). We denote $Q^\star_{\rm R}$ and $\Pi^\star_{\rm G}$ the critical values of $Q_{\rm R}$ and $\Pi_{\rm G}$, that is, their value at the boundary between catastrophic and erosive collision. We have

$$Q^\star_{\rm R} = \Pi^\star_{\rm G} \left(\rho \mathcal{G}\right)^{3\mu/2} R_2^{3\mu} \Delta v^{2-3\mu}. \tag{70}$$

7.3.2 Numerical estimates

We define the ejected mass $\check{m}$ as the total mass not pertaining to the largest fragment, that is (Suetsugu *et al.*, 2018, Eq. (2))

$$\check{m} = M - \tilde{m}. \tag{71}$$

In the regime $Q_{\rm R} \sim Q^\star_{\rm R}$, Stewart and Leinhardt (2009), with SPH simulations, and Suetsugu *et al.* (2018), with purely hydrodynamics simulations, showed that Eq. (69) can be fitted by

$$\frac{\check{m}}{M} = \frac{1}{2}\frac{Q_{\rm R}}{Q^\star_{\rm R}}. \tag{72}$$

In the erosive regime ($Q_{\rm R} \ll Q^\star_{\rm R}$), a linear fit still holds and Suetsugu *et al.* (2018) find

$$\frac{\check{m}}{M} = \frac{\psi}{2}\frac{Q_{\rm R}}{Q^\star_{\rm R}}, \tag{73}$$

where, for frontal collisions ($\theta = 0$), $\psi = 0.4$. Both ψ and $Q^\star_{\rm R}$ depend on θ, but the value of ψ does not matter since $Q^\star_{\rm R}$ is proportional to ψ (Eq. (78)). If $Q_{\rm R} > 2\,Q^\star_{\rm R}$, then Eq. (73) predicts that the largest fragment has a mass 0 and this equation is not valid for very catastrophic collisions. When $Q_{\rm R}$ exceeds $1.8\,Q^\star_{\rm R}$ (Or equivalently, when $\tilde{m} \leq 0.1\,M$), the largest mass $\tilde{m}$ is no longer proportional to $Q_{\rm R}$, but rather follows an exponential law given by Eq. (44) of Leinhardt and Stewart (2012)

$$\frac{\tilde{m}}{M} = \frac{1.8^{3/2}}{10}\left(\frac{Q_{\rm R}}{Q^\star_{\rm R}}\right)^{-3/2}, \tag{74}$$

where the choice of the proportionality coefficient ensures the continuity with Eq. (73). The results of Sect. (7.3.4) about the fragments sizes distribution assume $\tilde{m} \propto Q_\mathrm{R}$. For simplifications, we consider in this study that in the super-catastrophic regime (when $Q_\mathrm{R} \geq 1.8\, Q^\star_\mathrm{R}$), only the largest fragment remains, and the rest of the mass is removed from the simulation and added to the inner fluid disk.

7.3.3 Mass of the largest fragment

Let $M(v)$ denote the total mass of fragment having a velocity (relative to the barycenter of the impactor and target) larger than v. We can use the knowlegde of the distribution of $M(v)$ to constrain the value of $\Pi^\star_\mathrm{G}$ in Eq. (70). Indeed, given how the largest remaining fragment is precisely defined (See end of Sect. 2 of Suetsugu *et al.*, 2018), we have

$$\check{m} = M(v_\mathrm{esc}), \tag{75}$$

where v_esc is the escape velocity of the sum target + impactor. The velocity distribution is given by (Housen and Holsapple, 2011, Table 1, Suetsugu *et al.*, 2018, Eq. (19))

$$\frac{M(v)}{m_1} = \frac{3k}{4\pi} C_1^{3\mu} \left(\frac{v}{\Delta v \cos\theta} \right)^{-3\mu}, \tag{76}$$

where k and C_1 are constants depending on the material properties. For liquid moonlets, Table 3 of Housen and Holsapple (2011) gives

$$\mu = 0.55, \qquad k = 0.2, \qquad C_1 = 1.5. \tag{77}$$

For rocky moonlets, μ and C_1 are unchanged but k increases to 0.3. Combining Eqs. (73) and (76), we obtain

$$\frac{Q^\star_\mathrm{R}}{v_\mathrm{esc}^2} = \frac{\psi\pi}{3k} \frac{m_2}{M} \left(C_1 \cos\theta\right)^{-3\mu} \left(\frac{\Delta v}{v_\mathrm{esc}} \right)^{2-3\mu}, \tag{78}$$

and so, with Eq. (70)

$$\Pi^\star_\mathrm{G} = \frac{m_2}{M} \frac{\psi\pi}{3k} \left(\frac{8\pi}{3} \right)^{3\mu/2} \left(C_1 \cos\theta\right)^{-3\mu}. \tag{79}$$

Combining Eqs. (66), (73) and (78), we have the final expression for the ejected mass

$$\frac{\check{m}}{m_1} = \frac{3k}{4\pi} C_1^{3\mu} \left(\frac{\Delta v \cos\theta}{v_\mathrm{esc}} \right)^{3\mu} \tag{80}$$

and the mass $\tilde{m}$ of the largest fragment follows directly from $\tilde{m} = M - \check{m}$.

7.3.4 Mass of the n^{th} largest fragment

Equation (80) gives the mass of the largest fragment, and in this section, we give an estimate of the mass of the n^{th} largest fragment for $n \geq 2$. Leinhardt and Stewart (2012) give for the size distribution of the moonlet fragments

$$n(r) = C r^{-(\beta+1)}, \tag{81}$$

where $n(r)dr$ is the total number of fragments with radii between r and $r+dr$, and C and β are constant. Let $\tilde{m}_n$ be the mass of the n^{th} largest fragment, and r_n its radius. We assume that all fragments are spherical with density ρ and we write $\tilde{m}_1 = \tilde{m}$.

Leinhardt and Stewart, 2012 (Sect. 3.2) use Eq. (81) to estimate $\tilde{m}_2$. Here we use use Eq. (81) to give an estimate of $\tilde{m}_n$ for all $n \geq 2$. The total number of fragments larger than the n^{th} largest fragment is

$$n = \int_{r_n}^{+\infty} n(r)dr = \frac{C}{\beta} r_n^{-\beta}, \quad \text{which gives} \quad r_n = \left(\frac{n\beta}{C}\right)^{-1/\beta}. \tag{82}$$

The total mass of fragments smaller than the n^{th} largest fragment is given by

$$M - \sum_{k=1}^{n-1} \tilde{m}_k = \int_0^{r_n} \frac{4}{3}\pi\rho r^3 n(r)dr = \frac{4\pi\rho C r_n^{3-\beta}}{3\,(3-\beta)}. \tag{83}$$

Equations (82) and (83) show that a realistic description verifies $0 < \beta < 3$. Combining these two equations, we obtain, for $n \geq 2$, the mass of the n^{th} largest fragment as

$$\frac{\tilde{m}_n}{M} = \frac{1}{n\beta}\,(3-\beta)\left(1 - \sum_{k=1}^{n-1} \frac{\tilde{m}_k}{M}\right). \tag{84}$$

In their simulations, Leinhardt and Stewart (2012) use the mass of the second largest fragment to constrain β. Their best fit corresponds to

$$\beta = 2.85, \tag{85}$$

and we adopt this value in this work. In Table 1, we show the sequence $(\tilde{m}_n)$ for different choices of $\tilde{m}$. This approach predicts an infinite number of fragments, and Table 1 shows

$\tilde{m}$	$10^3\tilde{m}_2$	$10^3\tilde{m}_3$	$10^3\tilde{m}_4$	$10^3\tilde{m}_5$	$10^3\tilde{m}_6$	$10^3\tilde{m}_{1000}$	$\tilde{m}_1 + \cdots + \tilde{m}_{1000}$
0.1	23.68	15.37	11.33	8.943	7.374	0.034	0.361
0.2	21.05	13.67	10.07	7.950	6.555	0.030	0.432
0.5	13.16	8.541	6.293	4.969	4.097	0.019	0.645
0.8	5.263	3.416	2.517	1.987	1.639	0.007	0.858
0.98	0.526	0.342	0.252	0.199	0.164	0.001	0.986

Table 1 — Sequence of the $\tilde{m}_n$ for different choices of the largest mass $\tilde{m}$. The $\tilde{m}_n$ have been normalized by M and $\beta = 2.85$.

that the total normalized mass $(\tilde{m}_1 + \cdots + \tilde{m}_n)/M$ tends slowly to 1 as n goes to infinity. Some truncation rule on the fragment sizes has to be defined to prevent a too large number of fragments. We detail it in Sect. 7.3.5

Asymptotic expansion ***This part is not used by the code. Refer to Sect. 7.3.5***

Equation (84) gives the mass of the n^{th} largest fragment, but it is a recurrence relation over all $n-1$ larger fragments. By induction, we can however show that the mass of the n^{th} largest fragment is given, for $n \geq 2$, by

$$\tilde{m}_n = \frac{\mathfrak{K}}{n}\,\check{m}\left(1 - \frac{\mathfrak{K}}{2}\right)\left(1 - \frac{\mathfrak{K}}{3}\right)\cdots\left(1 - \frac{\mathfrak{K}}{n-1}\right), \tag{86}$$

where $\check{m}$ is given by Eq. (80) and $\mathfrak{K} = (3-\beta)/\beta$. While this expression does not depend on $\tilde{m}_k$ for $k < n$, it is still not very tractable. We now find an asymptotic expansion of Eq. (86) that gives $\tilde{m}_n$ in a straightforward manner. Let $(V_n)_{n\geq 2}$ be the sequence

$$V_n = \left(1-\frac{\mathfrak{K}}{2}\right)\left(1-\frac{\mathfrak{K}}{3}\right)\cdots\left(1-\frac{\mathfrak{K}}{n}\right) = \prod_{j=2}^{n}\left(1-\frac{\mathfrak{K}}{j}\right). \tag{87}$$

Denoting $U_n = \ln V_n$, a comparison with the integral $\int_2^n \ln(1-\mathfrak{K}/x)dx$ yields $U_n \sim -\mathfrak{K}\ln n$. Hence there exists constants γ, $\mathfrak{a}'$, $\mathfrak{b}'$ and $\mathfrak{c}'$ such that the sequence $(U_n)_{n\geq 2}$ has the asymptotic expansion

$$U_n = -\mathfrak{K}\ln n + \gamma + \frac{\mathfrak{a}'}{n} + \frac{\mathfrak{b}'}{n^2} + \frac{\mathfrak{c}'}{n^3} + \mathcal{O}\left(\frac{1}{n^4}\right). \tag{88}$$

Defining $U'_n = U_n + \mathfrak{K}\ln n - \gamma$, the coefficients $\mathfrak{a}$, $\mathfrak{b}$ and $\mathfrak{c}$ are found by writing

$$U'_n - U'_{n+1} = \mathfrak{a}'\left(\frac{1}{n}-\frac{1}{n+1}\right) + \mathfrak{b}'\left(\frac{1}{n^2}-\frac{1}{(n+1)^2}\right) + \mathfrak{c}'\left(\frac{1}{n^3}-\frac{1}{(n+1)^3}\right) + \mathcal{O}\left(\frac{1}{n^5}\right). \tag{89}$$

Expanding both sides to fourth order in $1/n$, we obtain

$$\mathfrak{a}' = \frac{(3-\beta)(3-2\beta)}{2\beta^2}, \qquad \mathfrak{b}' = \frac{(3-\beta)(2-\beta)(3-2\beta)}{4\beta^3}, \qquad \mathfrak{c}' = \frac{\mathfrak{a}'^2}{3}. \tag{90}$$

The constant γ can be found numerically. We have

$$\gamma = 0.0213485661094397 \quad \Rightarrow \quad e^{\gamma} = 1.021578077080539. \tag{91}$$

Using $\tilde{m}_n = \mathfrak{K}\check{m}\,V_{n-1}/n$, we have for the mass of the n^{th} largest fragment

$$\tilde{m}_n = \frac{3-\beta}{\beta} e^{\gamma}\,\check{m}\,n^{-3/\beta}\left(1+\frac{\mathfrak{a}}{n}+\frac{\mathfrak{b}}{n^2}+\frac{\mathfrak{c}}{n^3}+\mathcal{O}\left(\frac{1}{n^4}\right)\right), \tag{92}$$

where

$$\begin{aligned}
\mathfrak{a} &= \frac{3(3-\beta)}{2\beta^2} \approx 0.02770083102493073,\\
\mathfrak{b} &= \frac{(3-\beta)(3+\beta)(9-2\beta)}{8\beta^4} \approx 0.005486452682223121,\\
\mathfrak{c} &= \frac{3(3-\beta)^2(3+\beta)(3+2\beta)}{16\beta^6} \approx 0.0004006726965108799.
\end{aligned} \tag{93}$$

In order to check the quality of the expansion, we denote $\tilde{m}_n$ the exact mass of the n^{th} largest fragment, obtained from Eq. (84) or (86), and $\tilde{m}'_n$ the asymptotic value given by Eq. (92). We give in Table 2 the relative error $|\tilde{m}_n - \tilde{m}'_n|/\tilde{m}_n$ between the exact expression and the asymptotic expression. The agreement is excellent for all $n \geq 2$.

n	2	3	4	10	100
$\dfrac{\lvert\tilde{m}_n - \tilde{m}'_n\rvert}{\tilde{m}_n}$	$2.38\,10^{-5}$	$4.90\,10^{-6}$	$1.57\,10^{-6}$	$4.06\,10^{-8}$	$4.04\,10^{-12}$

Table 2 — relative error $\lvert\tilde{m}_n - \tilde{m}'_n\rvert / \tilde{m}_n$ for different values of n.

7.3.5 A simple yet realistic collisional model

The fragmentation model described above predicts an infinite total number of fragments. In order to efficiently simulate the Moon forming disk, we need to define a truncation rule that prevents the total number of moonlets in the simulation from growing too fast. Since the partial mass $\tilde{m}_1 + \tilde{m}_2 + \cdots + \tilde{m}_n$ slowly converges to M as n goes to infinity (see Table 1), we cannot simply consider the first few largest fragments and discard the rest, as it would yield a huge mass loss.

We define the fragment tail as all the fragments but the largest. The mass of the fragment tail is thus the total ejected mass $\check{m}$. According to Eq. (84) or (86), the mass of the second largest fragment is

$$\tilde{m}_2 = \frac{3-\beta}{2\beta}\check{m}. \tag{94}$$

If we were to consider that the tail is composed of $\tilde{N}$ fragments all of mass $\tilde{m}_2$, then the tail would be made up of

$$\tilde{N} = \frac{2\beta}{3-\beta} = 38 \text{ moonlets if } \beta = 2.85. \tag{95}$$

This is already a lot, and in order not to overcomplicate, we simply assume that the tail is composed of $\tilde{N}$ moonlets of mass $\tilde{m}_2$ each. The final collisional model is as follow

- I define a mass threshold $m^{(0)}$ (say $10^{-7} M_{☾}$), such that if $\tilde{m}_2 < m^{(0)} \leq \tilde{N}\tilde{m}_2$, then the tail is made up of one unique fragment of mass $\tilde{N}\tilde{m}_2 = \check{m}$ and velocity $\check{v}$ given by Eq. (105). If $\check{m} < m^{(0)}$, then the collision results in a perfect merger.
- If $\tilde{m}_2 \geq m^{(0)}$, then the collision is resolved with the fragmentation model. The two moonlets are thus broken into $\tilde{N}+1$ pieces, where the largest fragment has a mass $\tilde{m} = m_1 + m_2 - \check{m}$ with $\check{m}$ given by Eq. (80), and the $\tilde{N}$ other fragments have a mass $\tilde{m}_2$ given by Eq. (94).
- For super-catastrophic events ($Q_{\mathrm{R}} \geq 1.8\, Q^{\star}_{\mathrm{R}}$), the mass of the largest fragment is given by Eq. (74). The other fragments are discarded and their mass added to the inner fluid disk.
- The largest fragment has velocity $\tilde{\boldsymbol{v}}$ and position $\tilde{\boldsymbol{r}}$ worked out in Sect. 7.3.8, while the $\tilde{N}$ other fragments have scalar velocities $\tilde{v}_1$, $\tilde{v}_2$, $\cdots$, $\tilde{v}_{\tilde{N}}$ given by Eq. (103), and directions defined in Sect. 7.3.7.
- The user chooses a threshold N_{max} for the total number of moonlets N that the simulation can handle. If N reaches N_{max}, then either the code raises an error, or the 5 % smallest moonlets are removed from the simulation and their mass added to the inner fluid disk.

- The value $\beta = 2.85$ should correspond to the most physically realistic choice, as it corresponds to the best fit of Leinhardt and Stewart (2012). However, it yields $\tilde{N} = 38$ which is quite large. If N reaches $N_{\max}$ too often, then a smaller value for β will need to be chosen. $\beta = 30/11 \Leftrightarrow \tilde{N} = 20$ could be more manageable.
- The conservation of the total angular momentum is achieved in Sect. 7.3.8

7.3.6 Velocities of fragments

We now estimate the velocities of the fragments after the impact. We assume the distribution of Housen and Holsapple (2011), given in Eq. (76), where $M(v)$ denotes the total mass of fragments with a speed larger than v.

Velocity of the largest fragment *Deprecated. Refer to Sect. 7.3.8*

According to Leinhardt and Stewart, 2012 (Sect. 3.3), the largest fragment has a velocity close to its initial velocity if the impact angle was large; and moves with the center of mass after a head-on collision. Therefore we write for the velocity of the largest fragment

$$\tilde{\boldsymbol{v}} = \cos\theta\, \boldsymbol{v}_{\rm cm} + (1 - \cos\theta)\, \boldsymbol{v}_2, \tag{96}$$

where $\boldsymbol{v}_{\rm cm} = (m_1\boldsymbol{v}_1 + m_2\boldsymbol{v}_2)/M$ is the velocity of the center of mass.

Velocity of the other fragments

Let $m(v)dv$ denote the total mass of particles having a velocity with respect to the largest fragment between v and $v + dv$. We have

$$m(v) = -\frac{dM(v)}{dv} = \frac{9\mu k}{4\pi} \left(\Delta v C_1 \cos\theta\right)^{3\mu} v^{-(3\mu+1)}. \tag{97}$$

Combining with Eq. (80), this can be rewritten as

$$m(v)v = 3\mu \check{m} \left(\frac{v_{\rm esc}}{v}\right)^{3\mu}. \tag{98}$$

Since all $\tilde{N}$ fragments of the tail are unbounded to the center of mass, the slowest of these is made up of particles having velocities between $v_{\rm esc}$ and some velocity u_1. More generally, the $k^{\rm th}$ fastest fragment of the tail has a velocity $\tilde{v}_k$ with respect to the center of mass given by

$$\tilde{m}_2 \tilde{v}_k = \int_{u_{k-1}}^{u_k} m(v) v dv, \tag{99}$$

where $u_0 = v_{\rm esc}$, $u_{\tilde{N}} = +\infty$ and for all $k \leq \tilde{N}$, $u_{k-1} < \tilde{v}_k < u_k$. The speeds u_k are unknown, but they can be found by writing

$$\tilde{m}_2 = \int_{u_{k-1}}^{u_k} m(v) dv = \check{m} \left[\left(\frac{v_{\rm esc}}{u_{k-1}}\right)^{3\mu} - \left(\frac{v_{\rm esc}}{u_k}\right)^{3\mu} \right]. \tag{100}$$

If we define

$$z_k = \left(\frac{v_{\rm esc}}{u_k}\right)^{3\mu}, \tag{101}$$

then Eq. (100) yields $z_{k-1} - z_k = \tilde{m}_2/\check{m}$, that is

$$z_k = 1 - \frac{k}{\tilde{N}}, \quad \text{for } 0 \leq k \leq \tilde{N}. \tag{102}$$

Injecting Eq. (102) into Eq. (99), we obtain for the velocity of the k^{th} fastest fragment of the tail

$$\frac{\tilde{v}_k}{v_{\text{esc}}} = \frac{\tilde{N}}{\varsigma}\left[\left(1 - \frac{k-1}{\tilde{N}}\right)^{\varsigma} - \left(1 - \frac{k}{\tilde{N}}\right)^{\varsigma}\right], \tag{103}$$

where $\varsigma = (3\mu - 1)/3\mu = 13/33$. According to Eq. (103), the fastest fragment of the tail has a speed

$$\tilde{v}_{\tilde{N}} = \frac{\tilde{N}^{1-\varsigma}}{\varsigma} v_{\text{esc}} \approx 23.105\, v_{\text{esc}} \quad \text{if } \beta = 2.85. \tag{104}$$

Surprisingly enough, this is independent of Δv. When the threshold $\tilde{m}_2 \geq m^{(0)}$ is not met, then the tail is made up of one unique fragment whose scalar velocity is

$$\check{v} = \frac{1}{\check{m}} \int_{v_{\text{esc}}}^{+\infty} m(v) v dv = \frac{v_{\text{esc}}}{\varsigma} = \frac{33}{13} v_{\text{esc}}. \tag{105}$$

7.3.7 Direction of fragments

After the impact, the fragments of the tail are given positions and speeds with respect to the largest fragment according to the following schema.

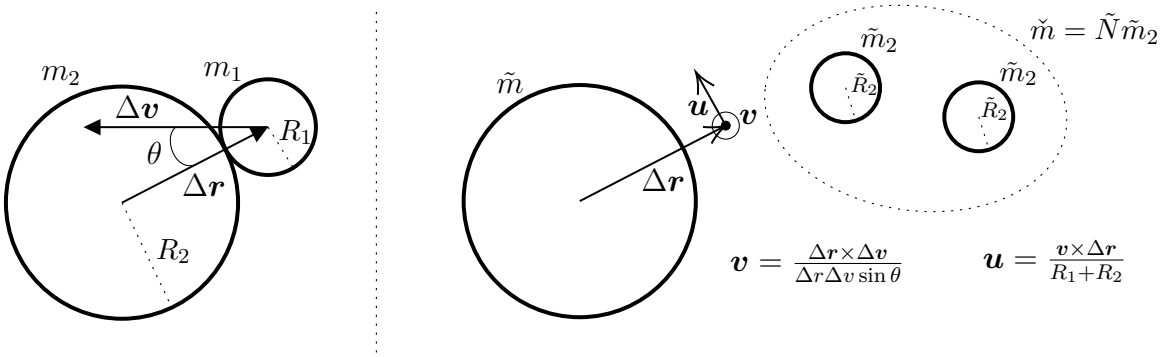

We give to the k^{th} fragment of the tail the position

$$\tilde{\boldsymbol{r}}'_k = \Delta \boldsymbol{r} + 2p_k \tilde{R}_2 \boldsymbol{u} + 2q_k \tilde{R}_2 \boldsymbol{v}, \tag{106}$$

and the speed

$$\tilde{\boldsymbol{v}}'_k = \tilde{v}_k \frac{\tilde{\boldsymbol{r}}'_k}{\tilde{r}'_k} = \tilde{v}_k \frac{\tilde{\boldsymbol{r}}'_k}{\sqrt{(R_1 + R_2)^2 + 4\tilde{R}_2^2 (p_k^2 + q_k^2)}}, \tag{107}$$

where $(p_k, q_k) \in \mathbb{Z}^2$ and $\tilde{v}_k$ is given by Eq. (103). If the collision is nearly frontal, then the vector $\boldsymbol{v}$ is ill-defined in this schema. In that case we take for $\boldsymbol{v}$ any unit vector orthogonal to $\Delta \boldsymbol{r}$. With $\tilde{N} = 15$ (or $\beta = 45/17$), $-1 \leq p_k \leq 3$ and[4] $-1 \leq q_k \leq 1$, the fragmented moonlets would look like

[4] This choice ensures that more fragments are ejected forward than backward, which sounds intuitive.

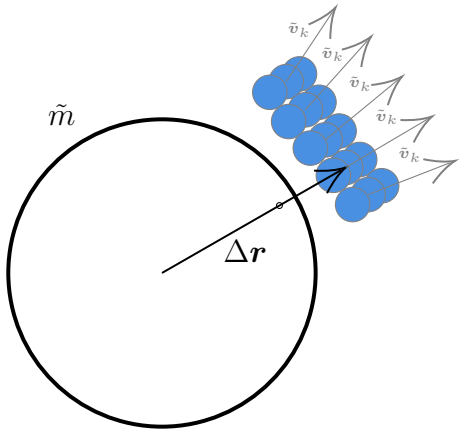

While all fragments of the tail are unbounded to the largest fragment, there is no reason why the fragments of the tail should be unbounded to one another. Depending on their relative velocities, some pairs will be unbounded while some others will not. With $\tilde{N} = 15$ the scalar velocities range from $\tilde{v}_1 \approx 1.02\, v_{\rm esc}$ to $\tilde{v}_{15} \approx 13.1\, v_{\rm esc}$, and considering that $v_{\rm esc}$ is the escape velocity at the surface of a complete merger, it is clear that most pairs, if not all, will be unbounded when $\check{m} \ll \tilde{m}$. If the tail is made up of one unique fragment, then we take $p_1 = q_1 = 0$.

7.3.8 Conservation of the total angular momentum

With the current fragmentation model, the total angular momentum is, a priori, not conserved upon impact. In this section, we choose the velocity $\tilde{\boldsymbol{v}}$ and the position $\tilde{\boldsymbol{r}}$ of the largest fragment in such a way that the total angular momentum is preserved upon impact. Then, the velocity and position of the $k^{\rm th}$ fragment of the tail are given in the geocentric reference frame $(\mathcal{O}, \boldsymbol{i}, \boldsymbol{j}, \boldsymbol{k})$ by

$$\tilde{\boldsymbol{r}}_k = \tilde{\boldsymbol{r}}'_k + \tilde{\boldsymbol{r}}, \quad \tilde{\boldsymbol{v}}_k = \tilde{\boldsymbol{v}}'_k + \tilde{\boldsymbol{v}}. \tag{108}$$

Case of a merger

If the collision results in a merger, then the outcome is a single moonlet of mass $M = m_1 + m_2$. The conservation of the total angular momentum reads

$$m_1 \boldsymbol{r}_1 \times \boldsymbol{v}_1 + m_2 \boldsymbol{r}_2 \times \boldsymbol{v}_2 := \boldsymbol{G} = M \tilde{\boldsymbol{r}} \times \tilde{\boldsymbol{v}}. \tag{109}$$

It is interesting to notice that it is impossible to preserve both the total momentum and the total angular momentum. Indeed, the conservation of the total angular momentum implies that $\tilde{\boldsymbol{v}}$ is orthogonal to $\boldsymbol{G}$. However, the conservation of the total momentum reads $M\tilde{\boldsymbol{v}} = m_1 \boldsymbol{v_1} + m_2 \boldsymbol{v_2} := M \boldsymbol{v}_{\rm cm}$, and since we have

$$M \boldsymbol{v}_{\rm cm} \cdot \boldsymbol{G} = m_1 m_2 \boldsymbol{v}_2 \cdot \Delta \boldsymbol{r} \times \Delta \boldsymbol{v}, \tag{110}$$

it is possible to conserve both the momentum and the angular momentum only if $\Delta \boldsymbol{r} \times \Delta \boldsymbol{v} = \boldsymbol{0}$, or equivalently, if the collision is frontal ($\theta = 0$). For oblique collisions, the only way to conserve both is to take into account the spin of the moonlets. However, taking into account the spin complexifies the treatment of collisions as well as the numerical implementation and slows down the code. Here, we choose to give up the conservation of

the total momentum, as it merely traduces into a small kick to the global center of mass. Instead, we preserve the total angular momentum.

In order to preserve the total angular momentum, we write

$$\tilde{\boldsymbol{r}} = \frac{m_1}{M}\boldsymbol{r}_1 + \frac{m_2}{M}\boldsymbol{r}_2 + \delta\tilde{\boldsymbol{r}} := \boldsymbol{r}_{\rm cm} + \delta\tilde{\boldsymbol{r}}, \tag{111}$$

and we choose the smallest possible value of $\delta\tilde{\boldsymbol{r}}$ that verifies

$$\boldsymbol{G}\cdot\tilde{\boldsymbol{r}} = \boldsymbol{G}\cdot\delta\tilde{\boldsymbol{r}} + \frac{m_1 m_2}{M}\boldsymbol{r}_2\cdot\Delta\boldsymbol{r}\times\Delta\boldsymbol{v} = 0. \tag{112}$$

Equation (112) is of the form $\mathfrak{a}\cdot\boldsymbol{w} = \mathfrak{b}$ with unknown $\boldsymbol{w} = \delta\tilde{\boldsymbol{r}}$. We are lead to minimize $|\boldsymbol{w}|^2$ under the constraint $\mathfrak{a}\cdot\boldsymbol{w} = \mathfrak{b}$. We write

$$\mathcal{L}(\lambda, \boldsymbol{w}) = |\boldsymbol{w}|^2 + \lambda\left(\mathfrak{a}\cdot\boldsymbol{w} - \mathfrak{b}\right), \tag{113}$$

where λ is a Lagrange multiplier. The gradient of $\mathcal{L}$ vanishes when $\boldsymbol{w} = \mathfrak{b}\mathfrak{a}/\mathfrak{a}^2$, and therefore we take

$$\delta\tilde{\boldsymbol{r}} = \frac{m_1 m_2}{M}\boldsymbol{r}_2\cdot\left(\Delta\boldsymbol{v}\times\Delta\boldsymbol{r}\right)\frac{\boldsymbol{G}}{G^2}. \tag{114}$$

Once $\tilde{\boldsymbol{r}}$ is known, Eq. (109) has the form $\boldsymbol{a}\times\boldsymbol{w} = \boldsymbol{b}$ with unknown $\boldsymbol{w} = \tilde{\boldsymbol{v}}$. Since $\boldsymbol{a}\cdot\boldsymbol{b} = 0$, this equation has solutions given by[5] $\boldsymbol{w} = \left(\boldsymbol{b}\times\boldsymbol{a}\right)/a^2 + \alpha\boldsymbol{a}$ for any $\alpha\in\mathbb{R}$. Therefore, we take

$$\tilde{\boldsymbol{v}} = \frac{1}{M\tilde{r}^2}\boldsymbol{G}\times\tilde{\boldsymbol{r}} + \alpha\tilde{\boldsymbol{r}}, \tag{115}$$

where we choose the real number α in order to minimize $|\tilde{\boldsymbol{v}} - \boldsymbol{v}_{\rm cm}|$, where $\boldsymbol{v}_{\rm cm}$ is the velocity of the center of mass. We have

$$|\tilde{\boldsymbol{v}} - \boldsymbol{v}_{\rm cm}|^2 = \alpha^2\tilde{r}^2 - 2\alpha\tilde{\boldsymbol{r}}\cdot\boldsymbol{v}_{\rm cm} + K, \tag{116}$$

where K does not depend on α, and the minimal value of $|\tilde{\boldsymbol{v}} - \boldsymbol{v}_{\rm cm}|$ is thus reached at $\alpha = \left(\tilde{\boldsymbol{r}}\cdot\boldsymbol{v}_{\rm cm}\right)/\tilde{r}^2$. Finally, we achieve the conservation of the total angular momentum by giving to the unique moonlet resulting from the merger the position and velocity

$$\begin{cases} \tilde{\boldsymbol{r}} = \boldsymbol{r}_{\rm cm} + \dfrac{m_1 m_2}{M}\boldsymbol{r}_2\cdot\left(\Delta\boldsymbol{v}\times\Delta\boldsymbol{r}\right)\dfrac{\boldsymbol{G}}{G^2}, \\ \tilde{\boldsymbol{v}} = \dfrac{1}{M\tilde{r}^2}\boldsymbol{G}\times\tilde{\boldsymbol{r}} + \dfrac{\tilde{\boldsymbol{r}}\cdot\boldsymbol{v}_{\rm cm}}{\tilde{r}^2}\tilde{\boldsymbol{r}}, \end{cases} \tag{117}$$

where $\boldsymbol{r}_{\rm cm}$ is the position of the center of mass.

Case of a fragmentation

If the collision results in a full fragmentation ($\tilde{m}_2 \geq m^{(0)}$), then the conservation of the total angular momentum reads

$$\boldsymbol{G} = \tilde{m}\tilde{\boldsymbol{r}}\times\tilde{\boldsymbol{v}} + \tilde{m}_2\sum_{k=1}^{\tilde{N}}\left(\tilde{\boldsymbol{r}} + \tilde{\boldsymbol{r}}'_k\right)\times\left(\tilde{\boldsymbol{v}} + \tilde{\boldsymbol{v}}'_k\right). \tag{118}$$

[5] This comes from $\boldsymbol{a}\times\left(\boldsymbol{b}\times\boldsymbol{a}\right) = a^2\boldsymbol{b} - \left(\boldsymbol{a}\cdot\boldsymbol{b}\right)\boldsymbol{a}$.

In the case of a partial fragmentation ($\tilde{m}_2 < m^{(0)} \leq \check{m}$), the tail is reunited into a single moonlet and the sum in Eq. (118) has only one term. I define[6]

$$\tilde{\boldsymbol{g}} = \tilde{m}_2 \sum_{k=1}^{\tilde{N}} \tilde{\boldsymbol{r}}'_k \times \tilde{\boldsymbol{v}}'_k, \qquad \tilde{\boldsymbol{s}} = \tilde{m}_2 \sum_{k=1}^{\tilde{N}} \tilde{\boldsymbol{r}}'_k, \qquad \tilde{\boldsymbol{u}} = \tilde{m}_2 \sum_{k=1}^{\tilde{N}} \tilde{\boldsymbol{v}}'_k, \tag{119}$$

and Eq. (118) can be rewritten

$$\boldsymbol{G} = M\tilde{\boldsymbol{r}} \times \tilde{\boldsymbol{v}} + \tilde{\boldsymbol{r}} \times \tilde{\boldsymbol{u}} + \tilde{\boldsymbol{s}} \times \tilde{\boldsymbol{v}} + \tilde{\boldsymbol{g}}, \tag{120}$$

with unknowns $\tilde{\boldsymbol{r}}$ and $\tilde{\boldsymbol{v}}$. If $\tilde{\boldsymbol{r}}$ is known, then $\tilde{\boldsymbol{v}}$ is given by the equation

$$\boldsymbol{a} \times \tilde{\boldsymbol{v}} = \boldsymbol{b}, \quad \text{where} \quad \boldsymbol{a} = M\tilde{\boldsymbol{r}} + \tilde{\boldsymbol{s}} \ \text{ and } \ \boldsymbol{b} = \boldsymbol{G} - \tilde{\boldsymbol{r}} \times \tilde{\boldsymbol{u}} - \tilde{\boldsymbol{g}}. \tag{121}$$

Equation (121) only has solutions if $\boldsymbol{a} \cdot \boldsymbol{b} = 0$, and we first constrain $\tilde{\boldsymbol{r}}$ with the equation $\boldsymbol{a} \cdot \boldsymbol{b} = 0$. Then, we obtain $\tilde{\boldsymbol{v}}$ from Eq. (121). There are infinitely many choices for both $\tilde{\boldsymbol{r}}$ and $\tilde{\boldsymbol{v}}$, and in each case we choose them in order to be as close as possible from the conservation of the total momentum. The conservation of the total momentum reads

$$\begin{aligned} \tilde{m}\tilde{\boldsymbol{r}} + \tilde{m}_2 \sum_{k=1}^{\tilde{N}} (\tilde{\boldsymbol{r}} + \tilde{\boldsymbol{r}}'_k) &= M\tilde{\boldsymbol{r}} + \tilde{\boldsymbol{s}} = M\boldsymbol{r}_{\mathrm{cm}}, \\ \tilde{m}\tilde{\boldsymbol{v}} + \tilde{m}_2 \sum_{k=1}^{\tilde{N}} (\tilde{\boldsymbol{v}} + \tilde{\boldsymbol{v}}'_k) &= M\tilde{\boldsymbol{v}} + \tilde{\boldsymbol{u}} = M\boldsymbol{v}_{\mathrm{cm}}. \end{aligned} \tag{122}$$

In order to determine $\tilde{\boldsymbol{r}}$, we thus write $M\tilde{\boldsymbol{r}} + \tilde{\boldsymbol{s}} = M\left(\boldsymbol{r}_{\mathrm{cm}} + \delta\tilde{\boldsymbol{r}}\right)$ and we choose the smallest $\delta\tilde{\boldsymbol{r}}$ that verifies $\boldsymbol{a} \cdot \boldsymbol{b} = 0$. We have

$$\boldsymbol{a} \cdot \boldsymbol{b} = (M\tilde{\boldsymbol{r}} + \tilde{\boldsymbol{s}}) \cdot (\boldsymbol{G} - \tilde{\boldsymbol{g}}) + \tilde{\boldsymbol{r}} \cdot (\tilde{\boldsymbol{s}} \times \tilde{\boldsymbol{u}}) = (\boldsymbol{r}_{\mathrm{cm}} + \delta\tilde{\boldsymbol{r}}) \cdot (M\boldsymbol{G} - M\tilde{\boldsymbol{g}} + \tilde{\boldsymbol{s}} \times \tilde{\boldsymbol{u}}) = 0. \tag{123}$$

We are left to minimize $|\delta\tilde{\boldsymbol{r}}|$ under a constraint of the form $\mathfrak{a} \cdot \delta\tilde{\boldsymbol{r}} = \mathfrak{b}$. This was already done in the merger case with the theory of Lagrange multiplier and we have

$$\delta\tilde{\boldsymbol{r}} = \frac{\mathfrak{b}\mathfrak{a}}{\mathfrak{a}^2} = -\frac{(\boldsymbol{r}_{\mathrm{cm}} \cdot \mathfrak{a})\,\mathfrak{a}}{\mathfrak{a}^2} \quad \text{where} \quad \mathfrak{a} = M\left(\boldsymbol{G} - \tilde{\boldsymbol{g}}\right) + \tilde{\boldsymbol{s}} \times \tilde{\boldsymbol{u}}. \tag{124}$$

Now that $\tilde{\boldsymbol{r}}$ is known, we can obtain $\tilde{\boldsymbol{v}}$ from Eq. (121). The solutions of Eq. (121) are given by[5]

$$\tilde{\boldsymbol{v}} = \frac{\boldsymbol{b} \times \boldsymbol{a}}{a^2} + \alpha\boldsymbol{a}, \tag{125}$$

where $\alpha \in \mathbb{R}$. We choose for the real number α the value that is closest from preserving the total momentum, that is, we choose the value of α that minimizes $|M\left(\tilde{\boldsymbol{v}} - \boldsymbol{v}_{\mathrm{cm}}\right) + \tilde{\boldsymbol{u}}|$ (see Eq. (122)). We have

$$\frac{1}{M^2}\left|M\left(\tilde{\boldsymbol{v}} - \boldsymbol{v}_{\mathrm{cm}}\right) + \tilde{\boldsymbol{u}}\right|^2 = a^2\alpha^2 - 2\alpha\left(\boldsymbol{v}_{\mathrm{cm}} - \frac{\tilde{\boldsymbol{u}}}{M}\right) \cdot \boldsymbol{a} + K, \tag{126}$$

where K does not depend on α and therefore, we choose

$$\alpha = \frac{\left(\boldsymbol{v}_{\mathrm{cm}} - \tilde{\boldsymbol{u}}/M\right) \cdot \boldsymbol{a}}{a^2}. \tag{127}$$

We uniquely determined $\tilde{\boldsymbol{r}}$ and $\tilde{\boldsymbol{v}}$ in such a way that the total angular momentum is conserved upon impact up to machine precision, whether the collision results in a merger or in a fragmentation.

[6] For a partial fragmentation, the sums are reduced to one term and $\tilde{m}_2$ has to be replaced by $\check{m}$.

References

Armitage, P. J. (2010). *Astrophysics of Planet Formation*. Cambridge University Press.

Barnes, J. and Hut, P. (1986). A Hierarchical O(N Log N) Force-Calculation Algorithm. *Nature*, 324, pp. 446–449.

Bentley and Ottmann (1979). Algorithms for Reporting and Counting Geometric Intersections. *IEEE Transactions on Computers*, C-28.9, pp. 643–647.

Benz, W. and Asphaug, E. (1999). Catastrophic Disruptions Revisited. *Icarus*, 142, pp. 5–20.

Boué, G., Correia, A. C. M. and Laskar, J. (2019). On Tidal Theories and the Rotation of Viscous Bodies. 82, pp. 91–98.

Genda, H. *et al.* (2017). Impact Erosion Model for Gravity-Dominated Planetesimals. *Icarus*, 294, pp. 234–246.

Goldreich, P. and Ward, W. R. (1973). The Formation of Planetesimals. *The Astrophysical Journal*, 183, pp. 1051–1062.

Holsapple, K. A. and Housen, K. R. (1986). Scaling Laws for the Catastrophic Collisions of Asteroids. *Memorie della Societa Astronomica Italiana*, 57, pp. 65–85.

Housen, K. R. and Holsapple, K. A. (2011). Ejecta from Impact Craters. *Icarus*, 211, pp. 856–875.

Ida, S. *et al.* (2020). Uranian Satellite Formation by Evolution of a Water Vapour Disk Generated by a Giant Impact. *Nature Astronomy*, 4, pp. 880–885.

Khuller, S. and Matias, Y. (1995). A Simple Randomized Sieve Algorithm for the Closest-Pair Problem. *Information and Computation*, 118.1, pp. 34–37.

Leinhardt, Z. M. and Stewart, S. T. (2012). Collisions between Gravity-dominated Bodies. I. Outcome Regimes and Scaling Laws. *The Astrophysical Journal*, 745, p. 79.

Nakajima, M. *et al.* (2022). Large Planets May Not Form Fractionally Large Moons. *Nature Communications*, 13, p. 568.

Rein, H. and Liu, S.-F. (2012). REBOUND: An Open-Source Multi-Purpose N-body Code for Collisional Dynamics. *Astronomy & Astrophysics*, 537, A128.

Salmon, J. and Canup, R. M. (2012). Lunar Accretion from a Roche-interior Fluid Disk. *The Astrophysical Journal*, 760, p. 83.

Stewart, S. T. and Leinhardt, Z. M. (2009). Velocity-Dependent Catastrophic Disruption Criteria for Planetesimals. *The Astrophysical Journal*, 691, pp. L133–L137.

Suetsugu, R. *et al.* (2018). Collisional Disruption of Planetesimals in the Gravity Regime with iSALE Code: Comparison with SPH Code for Purely Hydrodynamic Bodies. *Icarus*, 314, pp. 121–132.

Wahr, J. (1996). *Geodesy and Gravity*. Samizdat Press.